Structure and Thermoelectric Properties of the New Quaternary Bismuth Selenides $A_{1-x}M_{4-x}Bi_{11+x}Se_{21}$ (A = K and Rb and Cs; M = Sn and Pb)—Members of the Grand Homologous Series $K_m(M_6Se_8)_m(M_{5+n}Se_{9+n})$

Antje Mrotzek,[a] Duck-Young Chung,[a] Nishant Ghelani,[b] Tim Hogan,[b] and Mercouri G. Kanatzidis*[a]

Abstract: Several members of the new family $A_{1-x}M_{4-x}Bi_{11+x}Se_{21}$ (A = K, Rb, Cs; M = Sn, Pb) were prepared by direct combination of A_2Se, Bi_2Se_3, Sn (or Pb), and Se at 800 °C. The single-crystal structures of $K_{0.54}Sn_{3.54}Bi_{11.46}Se_{21}$, $K_{1.46}Pb_{3.08}Bi_{11.46}Se_{21}$, $Rb_{0.69}Pb_{3.69}Bi_{11.31}Se_{21}$, and $Cs_{0.65}Pb_{3.65}Bi_{11.35}Se_{21}$ were determined. The compounds $A_{1-x}M_{4-x}Bi_{11+x}Se_{21}$ crystallize in a new structure type with the monoclinic space group *C*2/m, in which building units of the Bi_2Te_3 and NaCl structure type join to give rise to a novel kind of three-dimensional anionic framework with alkali-ion-filled tunnels. The building units are assembled from distorted, edge-sharing (Bi,Sn)Se_6 octahedra. Bi and Sn/Pb atoms are disordered over the metal sites of the chalcogenide network, while the alkali site is not fully occupied. A grand homologous series $K_m(M_6Se_8)_m(M_{5+n}Se_{9+n})$ has been identified of which the compounds $A_{1-x}M_{4-x}Bi_{11+x}Se_{21}$ are members. We discuss here the crystal structure, charge-transport properties, and very low thermal conductivity of $A_{1-x}M_{4-x}Bi_{11+x}Se_{21}$.

Keywords: bismuth · selenium · semiconductors · structure elucidation · thermoelectric materials

Introduction

There is a strong interest in developing chemical concepts[1] for the design of new materials[2] with superior thermoelectric properties.[3] The efficiency of a thermoelectric material is assessed by the figure of merit $ZT = S^2\sigma/\kappa$ with the Seebeck coefficient *S*, the electrical conductivity σ, and the thermal conductivity κ. The best known materials are optimized Bi_2Te_3 alloys with a ZT of ~ 1.[4] Our approach focuses on an exploratory investigation of ternary and quaternary bismuth chalcogenides. The examples of $CsBi_4Te_6$[5, 6] and β-$K_2Bi_8Se_{13}$[6, 7] show that the modification of the Bi_2Te_3-type framework, by incorporation of alkali metals or A_2Q (A = K, Rb, Cs; Q = S, Se, Te) into Bi_2Te_3- and Bi_2Se_3-type frameworks, can lead to thermoelectric materials with promising properties. According to Slack's phonon glass electron crystal concept[1a,b] the alkali atoms can reduce the thermal conductivity by undergoing "rattling" motion in tunnels or cages in the anionic framework. However, the low crystal symmetry and structural complexity of these systems also play a crucial role in suppressing the thermal conductivity.

Encouraged by these results we expanded our synthetic investigations to the quaternary systems in order to study the effect of structural complexity and mass fluctuation on the physical properties. The investigation of the systems A/Pb/Bi/Se (A = K, Rb, Cs, Sr, Ba, Eu) led to the compounds $K_{1.25}Pb_{3.5}Bi_{7.25}Se_{15}$,[8] $RbPbBi_3Se_6$, α- and β-$CsPbBi_3Se_6$,[9] $Sr_2Pb_2Bi_6Se_{13}$,[6a] $Ba_3Pb_3Bi_6Se_{15}$,[10] $Ba_3PbBi_6Se_{13}$,[11] and $Eu_2Pb_2Bi_6Se_{13}$.[6a] They exhibit considerable structural diversity brought about by combining fragments excised out of the Bi_2Te_3 and NaCl structure types. $K_{1.25}Pb_{3.5}Bi_{7.25}Se_{15}$ is a member of a distinct class of quaternary solids with the general formula $A_{1+x}M_{4-2x}M'_{7+x}Se_{15}$ (A = K, Rb; M = Pb, Sn; M′ = Bi, Sb).[8] The same structure type is adopted also by $Ba_3Pb_3Bi_6Se_{15}$,[10] while the compounds $Sr_2Pb_2Bi_6Se_{13}$, $Ba_3PbBi_6Se_{13}$,[11] and $Eu_2Pb_2Bi_6Se_{13}$ [6] crystallize in the $Sr_4Bi_6Se_{13}$ structure type. The isostructural compounds, $RbPbBi_3Se_6$ and β-$CsPbBi_3Se_6$, have Bi_2Te_3-type slabs in which the alkali ions are incorporated. In contrast, α-$CsPbBi_3Se_6$ crystallizes in a three-dimensional structure that is related to galenobismute ($PbBi_2S_4$).[12] Pb atoms have the tendency to disorder with Bi atoms or alkali metal atoms on the same crystallographic sites depending on the local coordination environment. Site-occupancy disorder on a particular lattice position generates randomness of the mass, size, and charge of the atoms that can strongly scatter heat-carrying lattice phonons.

[a] Prof. M. G. Kanatzidis, Dr. A. Mrotzek, Dr. D.-Y. Chung
Department of Chemistry
and Center for Fundamental Materials Research
Michigan State University, East Lansing, MI 48824 (USA)
Fax: (+1) 517-353-1793
E-mail: kanatzid@cem.msu.edu

[b] Prof. T. Hogan, N. Ghelani
Department of Electrical Engineering
Michigan State University, East Lansing, MI 48824 (USA)

  0947-6539/01/0709-1915 $ 17.50+.50/0

Because $K_{1.25}Pb_{3.5}Bi_{7.25}Se_{15}$[8] is an encouraging thermoelectric material, we investigated the system K/Sn/Bi/Se for analogues. In addition to the isostructural $K_{1+x}Sn_{4-2x}Bi_{7+x}Se_{15}$,[8] we also discovered $K_{1-x}Sn_{5-x}Bi_{11+x}Se_{22}$[13] and $K_{1-x}Sn_{4-x}Bi_{11+x}Se_{21}$ and the isostructural analogues $Rb_{1-x}Sn_{4-x}Bi_{11+x}Se_{21}$, $Cs_{1-x}Sn_{4-x}Bi_{11+x}Se_{21}$, $K_{1-x}Pb_{4-x}Bi_{11+x}Se_{21}$, $Rb_{1-x}Pb_{4-x}Bi_{11+x}Se_{21}$, and $Cs_{1-x}Pb_{4-x}Bi_{11+x}Se_{21}$. We describe here the crystal structure, charge transport properties, and thermal conductivities of the new family $A_{1-x}M_{4-x}Bi_{11+x}Se_{21}$. We also place in perspective the relationship between these various families and other previously reported systems.

Results and Discussion

Structure description: The compounds $A_{1-x}M_{4-x}Bi_{11+x}Se_{21}$ (A = K, Rb, Cs; M = Sn, Pb) crystallize in a new structure type in the monoclinic space group *C*2/m with two formulas per unit cell. Figure 1 shows a (001) projection of the structure that is composed of two distinct building units derived from the Bi_2Te_3 and NaCl structure type, respectively. These building units, which are highlighted in Figure 2, are infinitely long in the *b* direction. They are arranged parallel to one another to form a three-dimensional anionic framework with straight tunnels, running along the *b* axis, filled partially by alkali metal atoms. The structure of $A_{1-x}M_{4-x}Bi_{11+x}Se_{21}$ (A = K, Rb, Cs, M = Sn, Pb) is closely related to that of $K_{1-x}Sn_{5-x}Bi_{11+x}Se_{22}$,[13] whose composition differs by one SnSe per formula unit. As depicted in Figure 2, both structure types have the similar building blocks but are arranged slightly different.

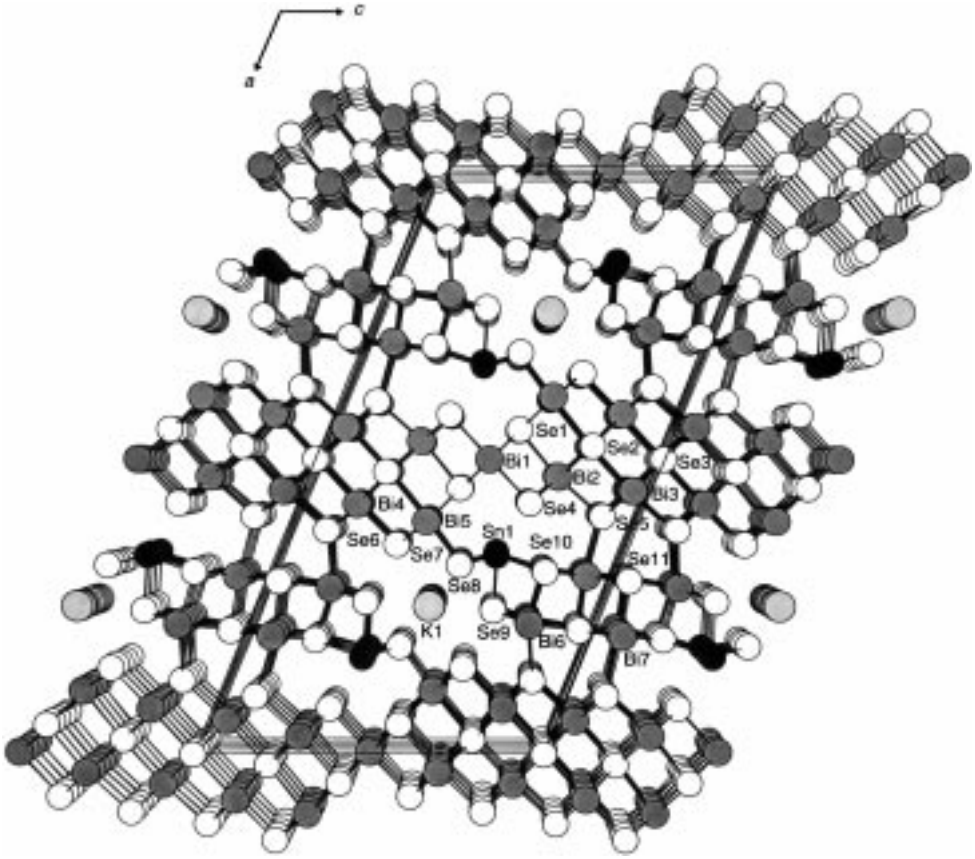

Figure 1. The structure of $K_{0.54}Sn_{3.54}Bi_{11.46}Se_{21}$ with atom labeling.

The following description is focused on $K_{0.54}Sn_{3.54}Bi_{11.46}Se_{21}$ and discusses the mixed occupancy of the Bi and Sn sites and its consequences. The analogous interatomic distances for the isostructural compounds $K_{1.46}Pb_{3.08}Bi_{11.46}Se_{21}$, $Rb_{0.69}Pb_{3.69}Bi_{11.31}Se_{21}$, $Cs_{0.65}Pb_{3.65}Bi_{11.35}Se_{21}$ can be found in Tables 4, 6, 8, and 10 in the Experimental Section.

The Bi_2Te_3 building units in the structure are five Bi octahedra wide along the *c* direction and they are joined in an offset

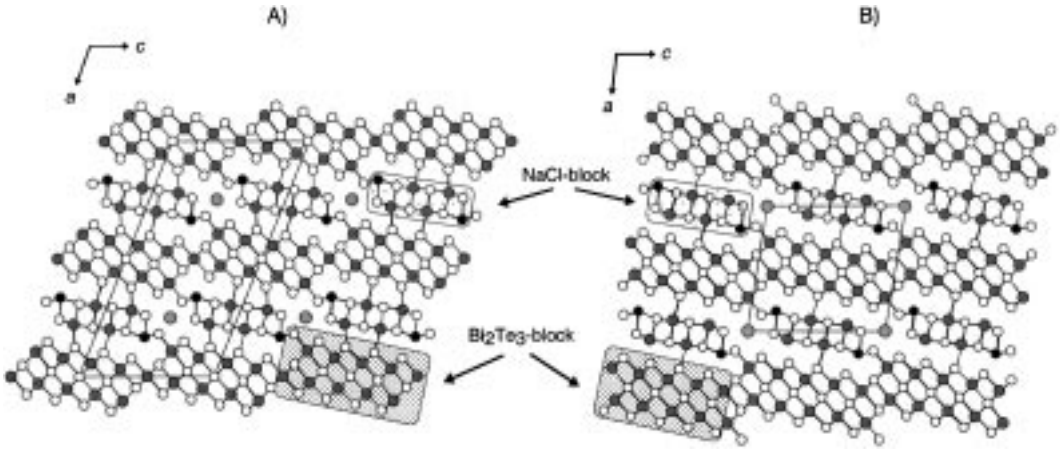

Figure 2. Comparison of the structure of $K_{0.54}Sn_{3.54}Bi_{11.46}Se_{21}$ (A) with the structure of $K_{0.66}Sn_{4.82}Bi_{11.18}Se_{22}$ (B) viewed down the *b* axis. Small white spheres: Se, large light-gray spheres: K, middle-gray spheres: Bi, black spheres: Sn. The archetypal Bi_2Te_3- and NaCl-type building units are highlighted as rectangular blocks in both structures.

0947-6539/01/0709-1916 $ 17.50+.50/0 *Chem. Eur. J.* **2001**, *7*, No. 9

fashion to form a step-shaped layer that extends in the *bc* plane. The connection point of these fragments is found at the octahedral Bi1 site. In contrast, the same building units, which are also offset, are joined through the *edge of an octahedron* in $K_{0.66}Sn_{4.82}Bi_{11.18}Se_{22}$,[13] see Figure 2. The lone pairs of the Bi^{3+} and Sn^{2+} atoms presumably cause a distorted coordination with three near and three more remote Se atoms in the edge-sharing $(Bi,Sn)Se_6$ octahedra. The interatomic (Bi,Sn)–Se distances range from 2.733(4) Å to 3.176(4) Å. The octahedral sites with a more regular coordination, Bi1, Bi2, and Bi4, are fully occupied by Bi. The Sn/Bi disorder is found in the more distorted sites Bi3 and Bi5, which contain 15% and 18% Sn, respectively. These sites connect the Bi_2Te_3-type layers with the NaCl-type blocks by common selenium atoms.

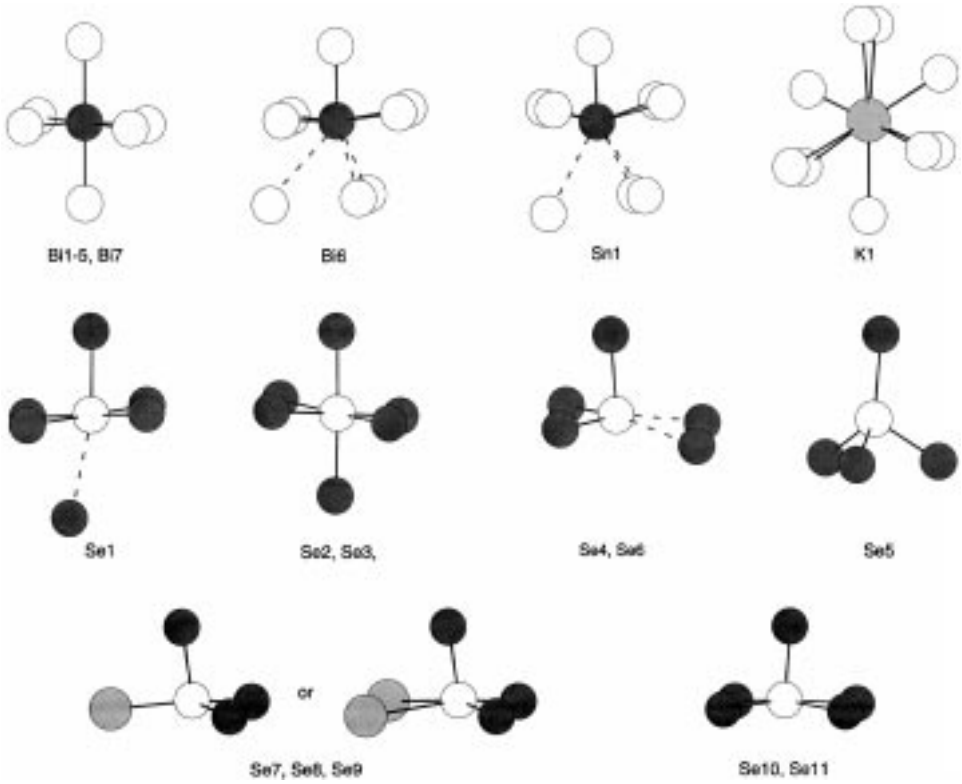

Figure 3. Local coordination environments of the metal and Se atoms in $K_{0.54}Sn_{3.54}Bi_{11.46}Se_{21}$. Small white spheres: Se, large light-gray spheres: K, middle-gray spheres: Bi, black spheres: Sn.

The NaCl-type blocks are identical to those found in the structure of $K_{1-x}Sn_{5-x}Bi_{11+x}Se_{22}$. These blocks are three Bi octahedra wide parallel to the direction of the Bi_2Te_3-type layers and one Bi octahedron high perpendicular to this direction. The NaCl-type blocks connect to the Bi_2Te_3-type blocks through M–Se interactions. All metal positions in this block show mixed Bi/Sn occupancy. The fraction of Sn increases at the periphery of the NaCl-type block. The Bi7 site has an extremely distorted octahedral coordination and contains 25% Sn. The sites Bi6 and Sn1 with 34% Sn and 16% Bi, respectively, are surrounded by selenium atoms in five-coordinate square-pyramidal environments. However, if the three more remote selenium atoms ($d_{Bi6-Se6} = 3.57$ Å ($\times 2$), $d_{Bi6-Se7} = 3.92$ Å ($\times 1$) and $d_{Sn1-Se4} = 3.75$ Å ($\times 2$), $d_{Sn1-Se1} = 3.85$ Å ($\times 1$)) are counted in the coordination sphere then we have a bi-capped trigonal prism. Typical coordination polyhedra are shown in Figure 3.[14] The different Bi/Sn distribution in the NaCl-type building units in $K_{0.54}Sn_{3.54}Bi_{11.46}Se_{21}$ and $K_{0.66}Sn_{4.82}Bi_{11.18}Se_{22}$ affects the average metal–Se distances. For example, consistent with the higher Sn content in the Bi6 and Bi7 sites in $K_{0.54}Sn_{3.54}Bi_{11.46}Se_{21}$ the mean Bi–Se bond lengths ($\bar{d} = 3.24$ Å, $\bar{d} = 2.94$ Å) are slightly shorter than in $K_{0.66}Sn_{4.82}Bi_{11.18}Se_{22}$ ($\bar{d} = 3.26$ Å, $\bar{d} = 2.95$ Å). A higher Bi fraction (16% Bi) in the Sn1 site in $K_{0.54}Sn_{3.54}Bi_{11.46}Se_{21}$ results in a greater distortion at this site with longer Sn1–Se bond lengths ($\bar{d} = 3.28$ Å) than in $K_{0.66}Sn_{4.82}Bi_{11.18}Se_{22}$ (11% Bi, $\bar{d} = 3.24$ Å).

The alkali metals are found in distorted tri-capped trigonal prismatic sites in the tunnels created by parallel arrangement of the Bi_2Te_3- and NaCl-type building units to a three-dimensional framework. The observed large atomic displacement parameters could be due to either "rattling" of the alkali atoms on their crystallographic sites or, more likely, positional disorder along the tunnel, since the position is only about 1/3 occupied.

Homologous series: The structure of $K_{1-x}Sn_{4-x}Bi_{11+x}Se_{21}$ is closely related to those of β-$K_2Bi_8Se_{13}$,[6, 7] $K_{2.5}Bi_{8.5}Se_{14}$,[15] $K_{1+x}Sn_{4-2x}Bi_{7+x}Se_{15}$,[8] and $K_{1-x}Sn_{5-x}Bi_{11+x}Se_{22}$.[13] The local environment of alkali metal ions, and the size of the NaCl- and Bi_2Te_3-type building units are very similar in $K_{1-x}Sn_{4-x}Bi_{11+x}Se_{21}$ and $K_{1-x}Sn_{5-x}Bi_{11+x}Se_{22}$, see Figure 2. Only the arrangement of the Bi_2Te_3-type units in a step-shaped layer is different in each compound. In $K_{1-x}Sn_{4-x}Bi_{11+x}Se_{21}$ the Bi_2Te_3-type blocks share one Bi atom, while the similar building units are connected through two common Se atoms in $K_{1-x}Sn_{5-x}Bi_{11+x}Se_{22}$. The relationship between the two compounds can be understood if the formulas are broken down into two parts, the anionic framework and the alkali metal cations in the tunnels. The K^+ ions stabilize the anionic framework where mixed site occupancies with Bi and Sn atoms are found. Therefore, the formula of $K_{1-x}Sn_{4-x}Bi_{11+x}Se_{21}$ can be written as $K^+[Sn_4Bi_{11}Se_{21}]^-$ or $K^+[M_{15}Se_{21}]^-$ (M = Sn + Bi in the anionic framework). Similarly $K_{1-x}Sn_{5-x}Bi_{11+x}Se_{22}$ can be expressed by $K^+[Sn_5Bi_{11}Se_{22}]^-$ or $K^+[M_{16}Se_{22}]^-$ (M = Sn + Bi in the anionic framework). Therefore a neutral "MSe" unit must be added to $K^+[M_{15}Se_{21}]^-$ to produce $K_{1-x}Sn_{5-x}Bi_{11+x}Se_{22}$ (or $K^+[M_{16}Se_{22}]^-$). A similar relationship[8] was found between β-$K_2Bi_8Se_{13}$,[6, 7] $K_{2.5}Bi_{8.5}Se_{14}$,[15] and $K_{1.25}Pb_{3.5}Bi_{7.25}Se_{15}$.[8] The latter are

derived by successively adding neutral "MSe" units to $K_2Bi_8Se_{13}$ (or $K^+[M_9Se_{13}]^-$) as follows:

$$K^+[M_9Se_{13}]^- \xrightarrow{[MSe]} K^+[M_{10}Se_{14}]^- \xrightarrow{[MSe]} K^+[M_{11}Se_{15}]^-$$

Furthermore, the structure of $K_{1+x}M_{4-2x}Bi_{7+x}Se_{15}$ (M = Sn, Pb) is closely related to that of $K_{1-x}Sn_{5-x}Bi_{11+x}Se_{22}$, as they possess the same type of step-shaped layer, but differ in the size of the NaCl-type units. To understand the relationship of these two families, we can break down the formula of the anionic framework of $K_{1-x}Sn_{5-x}Bi_{11+x}Se_{22}$ in two parts, one associated with the Bi_2Te_3-type layers and one representing the NaCl-type rods, as follows:

$$K^+[M_{16}Se_{22}]^- = K^+[\underset{\text{rod}}{M_6Se_8}]^-[\underset{\text{layer}}{M_{10}Se_{14}}]$$

Consequently, $K_{1+x}Sn_{4-2x}Bi_{7+x}Se_{15}$ is derived from $K_{1-x}Sn_{5-x}Bi_{11+x}Se_{22}$ by doubling the NaCl-type block, according to

$$K_2^{2+}[\underset{\text{rod}}{M_{12}Se_{16}}]^{2-}[\underset{\text{layer}}{M_{10}Se_{14}}] = K_2^{2+}[M_{22}Se_{30}]^{2-} = 2 \times K^+[M_{11}Se_{15}]^-$$

This is a useful relationship because it places five different structure types, β-$K_2Bi_8Se_{13}$, $K_{2.5}Bi_{8.5}Se_{14}$, $K_{1+x}Sn_{4-2x}Bi_{7+x}Se_{15}$, $K_{1-x}Sn_{4-x}Bi_{11+x}Se_{21}$, and $K_{1-x}Sn_{5-x}Bi_{11+x}Se_{22}$, in same context as shown in Figure 4. In fact all compounds are members of the homologous series $K_m(M_6Se_8)_m(M_{5+n}Se_{9+n})$. The different step-shaped layers of the selenides are derived by successively adding of MSe units to a (M_5Se_9) layer. Linking the layers by NaCl-type $(M_6Se_8)_m$ units generates the various structure types we observe.

It would be interesting to search for other homologues predicted by the $K_m(M_6Se_8)_m(M_{5+n}Se_{9+n})$ series. According to the scheme a compound with the formula, $K^+[M_{14}Se_{20}]^-$, charge-balanced with composition $KSn_3Bi_{11}Se_{20}$, is predicted to be a member. This hypothetical compound and $K_{2.5}Bi_{8.5}Se_{14}$ should show the same relationship as $K_{1+x}Sn_{4-2x}Bi_{7+x}Se_{15}$ does with $K_{1-x}Sn_{5-x}Bi_{11+x}Se_{22}$. We can also predict the charge-balanced formulas $KSnBi_{11}Se_{18}$ ($m = 1$, $n = 1$) and $K_2Sn_7Bi_{14}Se_{29}$ ($m = 2$, $n = 4$) as missing members of the homologous series $K_m(M_6Se_8)_m(M_{5+n}Se_{9+n})$. It would be worthwhile to attempt to prepare these compounds.

Charge transport properties and energy gaps: The temperature dependence of electrical conductivity and thermopower of $K_{1-x}Pb_{4-x}Bi_{11+x}Se_{21}$, $Rb_{1-x}Sn_{4-x}Bi_{11+x}Se_{21}$, $Rb_{1-x}Pb_{4-x}Bi_{11+x}Se_{21}$, and $Cs_{1-x}Pb_{4-x}Bi_{11+x}Se_{21}$ were measured on polycrystalline ingots, see Figures 5 and 6. Table 1 summarizes the room temperature values for the electrical conductivity of $A_{1-x}M_{4-x}Bi_{11+x}Se_{21}$ (A = K, Rb, Cs; M = Sn, Pb) and the thermopower obtained on polycrystalline samples between 300 and 400 K. The electrical conductivity of polycrystalline samples as a function of temperature are displayed in Figure 5. $Rb_{1-x}Pb_{4-x}Bi_{11+x}Se_{21}$ has the highest electrical conductivity with values starting around 1050 $S\,cm^{-1}$ at 80 K and falling to 530 $S\,cm^{-1}$ at 300 K. In comparison, the Sn analogue is less conductive with an electrical conductivity of 450 $S\,cm^{-1}$ at 80 K and 160 $S\,cm^{-1}$ at 400 K. The change from Rb to K or Cs causes a drop in the electrical conductivity to 150 $S\,cm^{-1}$ at 350 K for $Cs_{1-x}Pb_{4-x}Bi_{11+x}Se_2$ and, less drastic, to 230 $S\,cm^{-1}$ at 400 K for $K_{1-x}Pb_{4-x}Bi_{11+x}Se_2$. The electrical conductivity of these selenides is four orders of magnitude higher than that of the quaternary lead–bismuth selenides, $RbPbBi_3Se_6$ and β-$CsPbBi_3Se_6$ (both 0.3 $S\,cm^{-1}$ at room temperature), described earlier.[9] The observed temperature dependencies are similar in all four analogues consistent with the behavior of a degenerately doped semi-metal or a narrow band-gap semiconductor.

Table 1. Thermoelectric properties, band gaps and melting points for $A_{1-x}M_{4-x}Bi_{11+x}Se_{21}$ measured on polycrystalline samples.

	σ [$S\,cm^{-1}$]	$S_{300\,K}$ [$\mu V\,K^{-1}$]	$S_{400\,K}$ [$\mu V\,K^{-1}$]	power factor [$\mu W\,cm^{-1}\,K^{-2}$]	E_g [eV]	M.p. [°C]
$K_{1-x}Sn_{4-x}Bi_{11+x}Se_{21}$	1800	−52	−75	4.9	–	673
$Rb_{1-x}Sn_{4-x}Bi_{11+x}Se_{21}$	200	−51	−73	0.5	0.50	679
$Cs_{1-x}Sn_{4-x}Bi_{11+x}Se_{21}$	170	−69	−96	0.8	0.52	690
$K_{1-x}Pb_{4-x}Bi_{11+x}Se_{21}$	260	−19	−37	0.1	–	674
$Rb_{1-x}Pb_{4-x}Bi_{11+x}Se_{21}$[a]	530	−45	–	1.1	0.62	680
$Rb_{1-x}Pb_{4-x}Bi_{11+x}Se_{21}$[a]	250	−63	−80	1.0	0.62	680
$Cs_{1-x}Pb_{4-x}Bi_{11+x}Se_{21}$	160	−56	−73	0.5	0.62	687

[a] Different batches.

The compounds $A_{1-x}M_{4-x}Bi_{11+x}Se_{21}$ possess moderate Seebeck coefficients, see Table 1. Variable temperature thermopower data from polycrystalline ingots of $K_{1-x}Pb_{4-x}Bi_{11+x}Se_{21}$, $Rb_{1-x}Sn_{4-x}Bi_{11+x}Se_{21}$, $Rb_{1-x}Pb_{4-x}Bi_{11+x}Se_{21}$, and $Cs_{1-x}Pb_{4-x}Bi_{11+x}Se_{21}$ indicate negative Seebeck coefficients and nearly linear dependence, see Figure 6. With rising temperature, the Seebeck coefficient decreases from $-14\,\mu V\,K^{-1}$ at 75 K to $-72\,\mu V\,K^{-1}$ at 400 K for $Rb_{1-x}Sn_{4-x}Bi_{11+x}Se_{21}$ and $Cs_{1-x}Pb_{4-x}Bi_{11+x}Se_{21}$, respectively. We observed smaller Seebeck coefficients for $K_{1-x}Pb_{4-x}Bi_{11+x}Se_{21}$ and $Rb_{1-x}Pb_{4-x}Bi_{11+x}Se_{21}$ starting from $-4\,\mu V\,K^{-1}$ at 75 K to $-35\,\mu V\,K^{-1}$ at 400 K and from $-12\,\mu V\,K^{-1}$ at 75 K to $-45\,\mu V\,K^{-1}$ at 300 K, respectively. The change from a lighter alkali metal to a heavier one results in higher thermopower for $A_{1-x}Pb_{4-x}Bi_{11+x}Se_{21}$. However, due to different doping levels in the samples from preparation to preparation we occasionally observed even higher thermopower values, see Table 1. Therefore, we expect these compounds to be sensitive to doping and work to improve the charge transport properties is in progress. The Seebeck coefficients found here are significantly smaller than those of $RbPbBi_3Se_6$ ($-560\,\mu V\,K^{-1}$) and β-$CsPbBi_3Se_6$ ($-550\,\mu V\,K^{-1}$),[9] and this is consistent with the higher electrical conductivity. The negative values indicate n-type behavior with electrons as the dominant charge carriers.

The infrared absorption spectra of the compounds $A_{1-x}M_{4-x}Bi_{11+x}Se_{21}$ (A = K, Rb, Cs; M = Sn, Pb) were recorded at room temperature in the range of 0.1 to 0.7 eV. A typical spectrum of $Rb_{1-x}Sn_{4-x}Bi_{11+x}Se_{21}$ is shown in Figure 7, while the detected optical band gaps are summarized in Table 1. The band gaps of $K_{1-x}Sn_{4-x}Bi_{11+x}Se_{21}$ and $K_{1-x}Pb_{4-x}Bi_{11+x}Se_{21}$ could not be reliably determined. The narrow band gaps between 0.5 and 0.6 eV are consistent with the semiconducting behavior of $A_{1-x}M_{4-x}Bi_{11+x}Se_{21}$ (A = K, Rb, Cs; M = Sn, Pb) revealed by their charge transport properties. According to DTA experiments the compounds $A_{1-x}M_{4-x}Bi_{11+x}Se_{21}$ melt and recrystallize without structural change;the melting points are listed in Table 1.

0947-6539/01/0709-1918 $ 17.50+.50/0 *Chem. Eur. J.* **2001**, *7*, No. 9

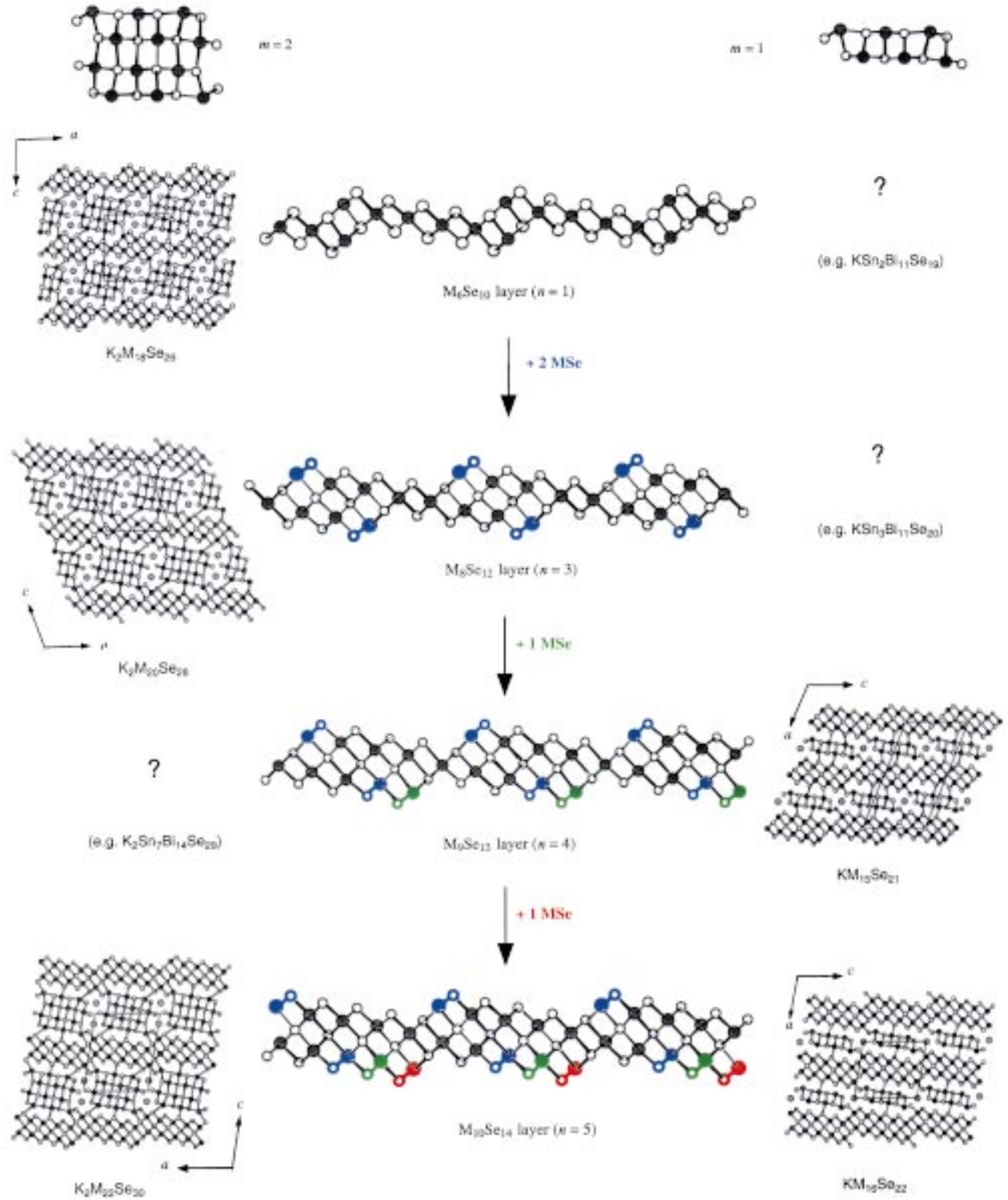

Figure 4. The homologous series $K_m(M_6Se_8)_m(M_{5+n}Se_{9+n})$. A member-generating scheme illustrating successive additions of MSe units to a M_5Se_9 layer. Small white spheres: Se, large light-gray spheres: K, middle-gray spheres: M.

Thermal conductivity: The temperature dependence of the thermal conductivity was measured on polycrystalline ingots of $K_{1-x}Pb_{4-x}Bi_{11+x}Se_{21}$, $Rb_{1-x}Sn_{4-x}Bi_{11+x}Se_{21}$, $Rb_{1-x}Pb_{4-x}Bi_{11+x}Se_{21}$, and $Cs_{1-x}Pb_{4-x}Bi_{11+x}Se_{21}$, and are shown in Figure 8. Except for $K_{1-x}Pb_{4-x}Bi_{11+x}Se_{21}$, which exhibits a slightly higher thermal conductivity, all samples possess very low thermal conductivity around 1 $W m^{-1} K^{-1}$ at room temperature. This is attributed collectively to the extensive disorder of the metal

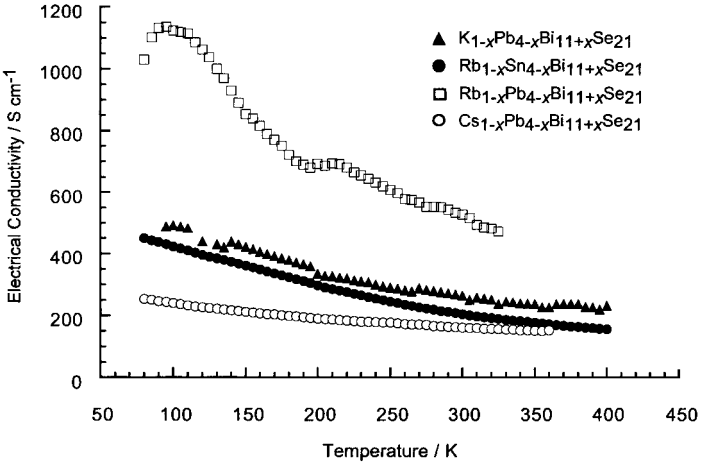

Figure 5. Variable-temperature electrical conductivity data from polycrystalline ingots of $K_{1-x}Pb_{4-x}Bi_{11+x}Se_{21}$, $Rb_{1-x}Sn_{4-x}Bi_{11+x}Se_{21}$, $Rb_{1-x}Pb_{4-x}Bi_{11+x}Se_{21}$, and $Cs_{1-x}Pb_{1-x}Bi_{11+x}Se_{21}$. The reason for the apparent metallic dependence of the electrical conductivity is the highly doped nature of the samples. Adventitious impurities act as dopands and give rise to a one-band conduction mechanism. This is common in narrow band semiconductors that include Bi_2Te_3.

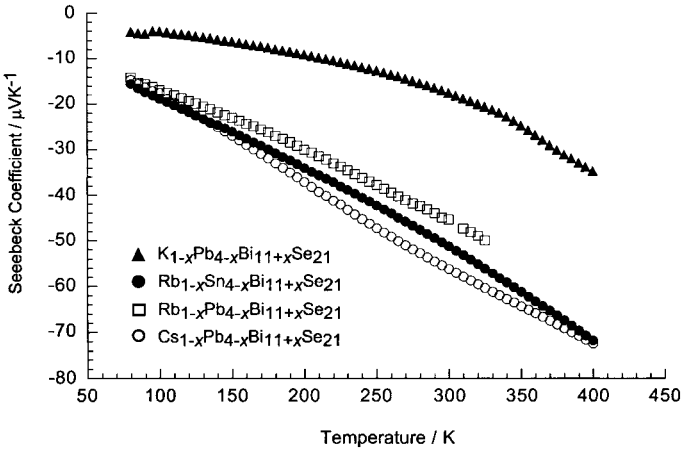

Figure 6. Variable-temperature thermoelectric power data from polycrystalline ingots of $K_{1-x}Pb_{4-x}Bi_{11+x}Se_{21}$, $Rb_{1-x}Sn_{4-x}Bi_{11+x}Se_{21}$, $Rb_{1-x}Pb_{4-x}Bi_{11+x}Se_{21}$, and $Cs_{1-x}Pb_{1-x}Bi_{11+x}Se_{21}$.

atoms in the anionic framework, the large unit cells, the low crystal symmetry, and possibly the "rattling" of the alkali ions in the tunnels of the chalcogenide framework. The observed values for $A_{1-x}M_{4-x}Bi_{11+x}Se_{21}$ are among the lowest reported for materials with potential thermoelectric interest. Optimized Bi_2Te_3 alloys have a thermal conductivity of $\sim 1.5\ W m^{-1} K^{-1}$, which is about 50% higher than those of $A_{1-x}M_{4-x}Bi_{11+x}Se_{21}$ (A = K, Rb, Cs; M = Sn, Pb). Because of their very low thermal conductivity it seems worthwhile to study systematically A-A′ or Pb-Sn solid solutions in order to enhance the thermoelectric properties.

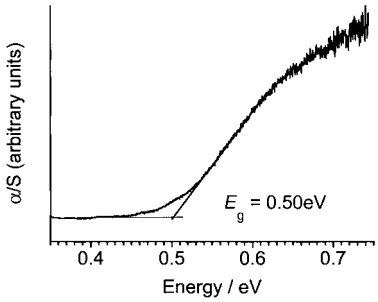

Figure 7. Infrared absorption spectrum of $Rb_{1-x}Sn_{4-x}Bi_{11+x}Se_{21}$ obtained at room temperature. The semiconductor band gap is indicated in the spectrum.

Conclusion

Synthetic investigations in the system A/M/Bi/Se with A = K, Rb, Cs and M = Sn, Pb revealed a new family of compounds, namely $A_{1-x}M_{4-x}Bi_{11+x}Se_{21}$, and a new structure type. Building units of the Bi_2Te_3 and NaCl structure type are the fundamental blocks that make up the novel anionic framework. The structure is related to those of β-$K_2Bi_8Se_{13}$, $K_{2.5}Bi_{8.5}Se_{14}$, $K_{1+x}M_{4-2x}Bi_{7+x}Se_{15}$, and $K_{1-x}Sn_{5-x}Bi_{11+x}Se_{22}$, all of which define a homologous series of the type $K_m(M_6Se_8)_m(M_{5+n}Se_{9+n})$. Extensive mixed occupancy is found between Bi and Sn (or Pb) in the metal sites of the

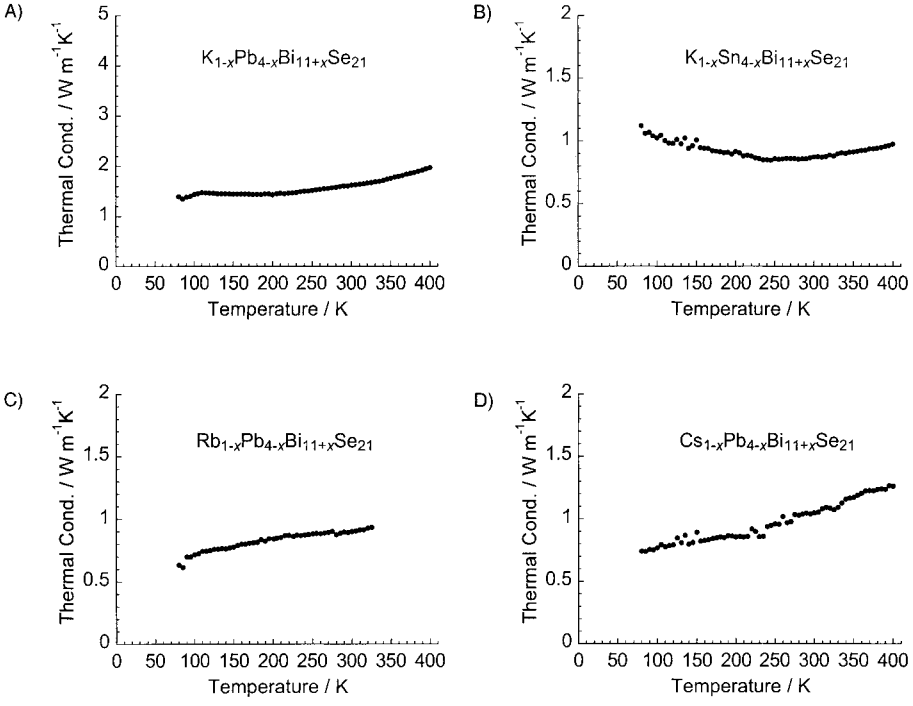

Figure 8. Variable-temperature thermal conductivity data from polycrystalline ingots of A) $K_{1-x}Pb_{4-x}Bi_{11+x}Se_{21}$, B) $Rb_{1-x}Sn_{4-x}Bi_{11+x}Se_{21}$, C) $Rb_{1-x}Pb_{4-x}Bi_{11+x}Se_{21}$, and D) $Cs_{1-x}Pb_{4-x}Bi_{11+x}Se_{21}$.

0947-6539/01/0709-1920 $ 17.50+.50/0 *Chem. Eur. J.* **2001**, *7*, No. 9

chalcogenide network; this may be responsible for the stability of the structure. This, together with the large, low symmetry unit cells and the possible "rattling" of alkali atoms, also gives rise to the remarkably low thermal conductivity of these compounds. These materials are n-type narrow band-gap semiconductors with moderate electrical conductivity and thermopower. Despite the moderate electrical conductivity and thermopower of $A_{1-x}M_{4-x}Bi_{11+x}Se_{21}$, their very low thermal conductivity makes them interesting for further investigations aimed to increase the thermoelectric power.

Experimental Section

Synthesis: All manipulations were carried out under a dry nitrogen atmosphere in a Vacuum Atmospheres Dri-Lab glovebox. Bi_2Se_3 was obtained by reaction of stoichiometric amounts of the elements (99.999% purity) in evacuated quartz glass ampoules at 800 °C for three days. K_2Se, Rb_2Se, and Cs_2Se were prepared by stoichiometric reaction of alkali metal and selenium in liquid ammonia.

$A_{1-x}M_{4-x}Bi_{11+x}Se_{21}$ (A = K, Rb, Cs; M = Sn, Pb): A mixture of A_2Se (0.5 mmol), Sn or Pb (4 mmol), Se (4 mmol), and Bi_2Se_3 (5.5 mmol) was loaded in a carbon-coated quartz tube (9 mm diameter) and sealed at a residual pressure of $< 10^{-4}$ Torr. The starting materials were heated over 24 hours to 800 °C and kept at this temperature for a further 24 hours, followed by slow cooling to 400 °C at a rate of 0.1 °C min^{-1} and then to 50 °C over a period of 10 hours. A silver, shiny, polycrystalline ingot of pure $A_{1-x}M_{4-x}Bi_{11+x}Se_{21}$ was obtained after washing away any impurities with dimethylformamide (DMF), methanol, and diethyl ether. Only $Cs_{1-x}Sn_{4-x}Bi_{11+x}Se_{21}$ was obtained in a mixture (70:30) with a compound of the composition "$Cs_{1-x}Sn_{5-x}Bi_{11+x}Se_{22}$".

A quantitative microprobe analysis with a SEM/EDS system, performed on different crystals, gave the average compositions $K_{0.5}Sn_{2.5}Bi_{11.8}Se_{21}$, $K_{1.0}Pb_{3.1}Bi_{11.3}Se_{21}$, $Rb_{1.9}Sn_{4.8}Bi_{10.3}Se_{21}$, $Rb_{0.8}Pb_{4.5}Bi_{10.7}Se_{21}$, $Cs_{0.8}Sn_{4.3}Bi_{10.6}Se_{21}$, and $Cs_{0.7}Pb_{4.5}Bi_{10.6}Se_{21}$.

Physical measurements

Electron microscopy: Quantitative microprobe analyses of the compounds were performed with a JEOL JSM-35C SEM equipped with a Tracer Northern energy dispersive spectroscopy (EDS) detector. Data were acquired by using an accelerating voltage of 25 kV and a 60 s accumulation time. The quantitative microprobe analyses have a standard deviation of about 2–5%.

Differential thermal analysis: Differential thermal analysis (DTA) was performed with a computer-controlled Shimadzu DTA-50 thermal analyzer. A sample of ground crystalline material (~20 mg total mass) was sealed in a carbon-coated silica ampoule under vacuum. A silica ampoule containing alumina of equal mass was sealed under vacuum and placed on the reference side of the detector. The sample was heated to 900 °C at 10 °C min^{-1}, maintained at this temperature for 5 min, cooled at 10 °C min^{-1} to 150 °C, and finally to room temperature by rapid cooling. Running multiple heating/cooling cycles monitored the stability/reproducibility of the sample. The DTA sample was examined by powder X-ray diffraction after the experiment.

Infrared spectroscopy: Diffuse reflectance measurements were made on finely ground samples at room temperature. The spectra were recorded in the region 6000–400 cm^{-1} with the use of a Nicolet MAGNA-IR 750 spectrometer equipped with a collector diffuse reflectance accessory from Spectra-Tech.[13]

Charge transport measurements: A four-sample measurement system was used to measure electrical conductivity, thermoelectric power, and thermal conductivity[16] of polycrystalline ingots. To fully characterize the figure of merit, these three properties were simultaneously measured for each sample over the selected temperature range of interest, that is, 77 K to 320 K (system capability is 4.2 K to 475 K). To alleviate offset error voltages and increase the density of data points, a slow ac-technique was used with a heater pulse period of 720 s.[17] The pulse shape was monitored, in situ, to determine temperature stabilization, and the sample chamber was maintained at a pressure less than 10^{-5} Torr for the entire measurement run. Samples were mounted in the standard four-probe configuration for both the electrical and thermal conductivity, and the heater current was adjusted for an average temperature gradient of 1 K. The sample stage and radiation shield were made of gold-coated copper to minimize radiation effects and maintain temperature uniformity. All electrical leads were 25 μm in diameter with lengths greater than 10 cm to minimize thermal conduction losses. Data acquisition and computer control of the system was maintained under the LabView™ software environment.

In addition, the Seebeck coefficient of polycrystalline samples was measured between 300 and 400 K by using a SB-100 Seebeck Effect Measurement System, MMR Technologies; room temperature conductivity measurements were performed in the usual four-probe geometry.

Powder X-ray diffraction: Powder patterns of all starting materials and products were obtained by using a Rigaku-Denki/Rw400F2 (rotaflex) rotating-anode powder diffractometer and a CPS 120 INEL X-ray powder

Table 2. Summary of crystallographic data and structural analysis.

formula	$K_{0.54}Sn_{3.54}Bi_{11.46}Se_{21}$	$K_{1.46}Pb_{3.08}Bi_{11.46}Se_{21}$	$Rb_{0.69}Pb_{3.69}Bi_{11.31}Se_{21}$	$Cs_{0.65}Pb_{3.65}Bi_{11.35}Se_{21}$
crystal habit	silver lath	silver lath	silver ribbon	silver lath
space group	*C*2/m	*C*2/m	*C*2/m	*C*2/m
a [Å]	31.910(8)	31.883(5)	31.991(5)	32.172(9)
b [Å]	4.146(1)	4.1863(7)	4.1937(7)	4.159(1)
c [Å]	17.311(4)	17.387(3)	17.481(3)	17.499(5)
β [°]	112.064(4)	112.098(3)	112.519(3)	112.672(6)
Z	2	2	2	2
V [Å^3]	2122.6	2150.2	2166.4	2160.5
ρ_{calc} [g cm^{-3}]	7.030	7.485	7.384	7.394
T [K]	293	293	293	293
λ ($Mo_{K\alpha}$) [Å]	0.71073	0.71073	0.71073	0.71073
μ ($Mo_{K\alpha}$) [cm^{-1}]	67.34	78.28	78.17	77.09
$2\theta_{max}$ [°]	57.43	56.98	57.45	56.45
relections measured	7828	8855	6684	12666
unique reflections	2755	2829	2845	2975
observed reflections [$I > 2\sigma(I)$]	1607	2267	1943	2039
parameters	128	121	116	119
final *R*1/*wR*2 [%][a]	5.37/8.98	5.83/11.53	5.00/9.24	4.63/8.52
largest difference peak/hole [e Å^{-3}]	2.33/ − 2.94	11.56/ − 3.54	3.89/ − 2.88	3.53/ − 3.21
goodness of fit	1.163	1.101	1.139	0.983

[a] $R1 = \Sigma||F_o| - |F_c||/\Sigma|F_o|$, $wR2 = \{\Sigma[w(F_o^2 - F_c^2)^2]/\Sigma[w(F_o^2)^2]\}^{1/2}$.

Table 3. Fractional atomic coordinates ($y=0$) and equivalent atomic displacement parameter (U_{eq})[a] values in 10^{-3} Å^2 for $K_{0.54}Sn_{3.54}Bi_{11.46}Se_{21}$ with estimated standard deviations in parentheses.

	x	z	occupancy	U_{eq}
Bi1	0.5	0.5	1	27.8(5)
Bi2	0.03080(5)	0.71839(8)	1	22.9(3)
Bi3/Sn3′	0.44520(5)	0.05262(8)	0.85(2)/0.15	21.5(5)
Bi4	0.07703(5)	0.17206(7)	1	21.6(3)
Bi5/Sn5′	0.39416(5)	0.60742(8)	0.82(2)/0.18	22.1(5)
Bi6/Sn6′	0.21984(5)	0.19477(9)	0.66(2)/0.34	25.4(5)
Bi7/Sn7′	0.19970(5)	0.91481(8)	0.75(2)/0.25	21.1(5)
Sn1/Bi1′	0.16477(9)	0.6326(1)	0.84(2)/0.16	39.2(9)
K1	0.250(3)	0.531(7)	0.27(4)	248(64)
Se1	0.0497(1)	0.4496(2)	1	22.6(8)
Se2	0.4786(1)	0.7793(2)	1	17.9(7)
Se3	0	0	1	20(1)
Se4	0.4249(1)	0.3340(2)	1	24.0(8)
Se5	0.0976(1)	0.8904(2)	1	24.5(8)
Se6	0.3782(1)	0.8809(2)	1	19.7(7)
Se7	0.1464(1)	0.3326(2)	1	20.7(7)
Se8	0.3199(1)	0.4617(2)	1	38(1)
Se9	0.2582(1)	0.6885(2)	1	29.4(9)
Se10	0.3083(1)	0.2105(2)	1	23.3(8)
Se11	0.2920(1)	0.9578(2)	1	20.1(7)

[a] U_{eq} is defined as one-third of the trace of the orthogonalized U_{ij} tensor.

Table 5. Fractional atomic coordinates ($y=0$) and equivalent atomic displacement parameter (U_{eq})[a] values in 10^{-3} Å^2 for $K_{1.46}Pb_{3.08}Bi_{11.46}Se_{21}$[b] with estimated standard deviations in parentheses.

	x	z	occupancy	U_{eq}
Bi1	0.5	0.5	1	19.7(3)
Bi2	0.02977(4)	0.72070(6)	1	19.0(3)
Bi/Pb3[c]	0.44492(4)	0.05131(6)	1	19.6(3)
Bi/Pb4[c]	0.07678(4)	0.17126(6)	1	17.9(3)
Bi5	0.39696(4)	0.60808(7)	1	24.4(3)
Bi6/K6′	0.22018(4)	0.19394(8)	0.887(8)/0.113	26.1(5)
Bi7/K7′	0.19984(4)	0.91786(8)	0.855(8)/0.145	20.8(4)
Pb/Bi1/K1′[c]	0.15572(7)	0.6392(1)	0.898(9)/0.102	41.3(6)
K1	0.248(2)	0.494(4)	0.37(4)	159(4)
Se1	0.0492(1)	0.4493(2)	1	19.6(6)
Se2	0.4785(1)	0.7793(2)	1	16.4(5)
Se3	0	0	1	16.4(8)
Se4	0.4266(1)	0.3336(2)	1	19.2(6)
Se5	0.0973(1)	0.8908(2)	1	21.0(6)
Se6	0.3783(1)	0.8805(2)	1	19.0(6)
Se7	0.1451(1)	0.3346(2)	1	20.7(6)
Se8	0.3272(1)	0.4575(2)	1	33.7(8)
Se9	0.2553(1)	0.6903(2)	1	27.5(7)
Se10	0.3087(1)	0.2061(2)	1	23.1(6)
Se11	0.2915(1)	0.9564(2)	1	21.2(6)

[a] U_{eq} is defined as one-third of the trace of the orthogonalized U_{ij} tensor. [b] Formula obtained according to charge balance requirements of the general formula $K_{1+x}Pb_{4-2x}Bi_{11+x}Se_{21}$. [c] Bond-valence calculations suggest that this position is most likely mixed occupied with Bi and Pb. Bi/Pb3 = 2.83, Bi/Pb4 = 2.83, Pb/Bi1/K1 = 2.44. Site Bi1, Bi2, Bi5, Bi6 and Bi7 gave >2.96.

Table 4. Selected interatomic distances [Å] for $K_{0.54}Sn_{3.54}Bi_{11.46}Se_{21}$. Because of the mixed Bi/Sn occupancy on all metal sites, these distances represent only average values.

Bi1	–Se1 × 4	2.935(2)	Bi2	–Se4 × 2	2.842(2)	Bi3	–Se5 × 2	2.855(2)
	–Se4 × 2	2.970(4)		–Se5	2.939(4)		–Se6	2.939(4)
				–Se1	3.073(4)		–Se2	3.011(4)
				–Se2 × 2	3.083(2)		–Se3 × 2	3.063(1)
Bi4	–Se7	2.829(4)	Bi5	–Se8	2.736(4)	Bi6	–Se10	2.733(4)
	–Se6 × 2	2.856(2)		–Se7 × 2	2.838(2)		–Se9 × 2	2.794(3)
	–Se2 × 2	3.046(2)		–Se1 × 2	3.132(2)		–Se11 × 2	3.266(3)
	–Se3	3.068(2)		–Se2	3.176(4)		–Se6 × 2	3.567(3)
							–Se7	3.924(3)
Bi7	–Se11	2.754(4)	Sn1	–Se9	2.766(5)	K1	–K1 × 2	2.073(1)
	–Se10 × 2	2.942(2)		–Se8 × 2	2.793(3)		–Se8	2.555(4)
	–Se11 × 2	2.965(2)		–Se10 × 2	3.264(3)		–Se9	3.175(3)
	–Se5	3.124(4)		–Se4 × 2	3.752(3)		–Se8 × 2	3.291(3)
				–Se1	3.845(4)		–Se7	3.484(4)
							–Se9 × 2	3.792(3)
							–Se7	4.054(3)
Se1	–Bi1 × 2	2.935(2)	Se2	–Bi3	3.011(4)	Se3	–Bi3 × 4	3.063(1)
	–Bi2	3.073(4)		–Bi4 × 2	3.046(2)		–Bi4 × 2	3.068(2)
	–Bi5 × 2	3.132(2)		–Bi2 × 2	3.083(2)			
	–Sn1	3.845(4)		–Bi5	3.176(4)			
Se4	–Bi2 × 2	2.842(2)	Se5	–Bi3 × 2	2.855(2)	Se6	–Bi4 × 2	2.856(2)
	–Bi1	2.970(4)		–Bi2	2.939(4)		–Bi3	2.939(4)
	–Se10	3.527(5)		–Bi7	3.124(4)		–Se11	3.478(4)
	–Sn1 × 2	3.751(3)					–Bi6 × 2	3.568(3)
Se7	–Bi4	2.829(4)	Se8	–K1	2.555(4)	Se9	–Sn1	2.766(5)
	–Bi5 × 2	2.838(2)		–Bi5	2.736(4)		–Bi6 × 2	2.794(3)
	–K1	3.484(4)		–Sn1 × 2	2.793(3)		–K1	3.175(3)
	–Se9 × 2	3.814(4)		–K1 × 2	3.291(3)		–Se8 × 2	3.523(4)
	–Se8 × 2	3.905(4)		–Se9 × 2	3.523(4)		–K1 × 2	3.792(3)
	–Bi6	3.924(3)		–Se7 × 2	3.905(4)		–Se7 × 2	3.814(4)
							–Se10 × 2	3.827(4)
Se10	–Bi6	2.733(4)	Se11	–Bi7	2.754(4)			
	–Bi7 × 2	2.942(2)		–Bi7 × 2	2.966(2)			
	–Sn1 × 2	3.264(3)		–Bi6 × 2	3.266(3)			
	–Se4	3.527(5)		–Se6	3.478(4)			
	–Se9 × 2	3.827(4)						

0947-6539/01/0709-1922 $ 17.50+.50/0 *Chem. Eur. J.* **2001**, *7*, No. 9

Table 6. Selected interatomic distances [Å] for $K_{1.46}Pb_{3.08}Bi_{11.46}Se_{21}$. Because of the mixed Bi/Pb occupancy on all metal sites, these distances represent only average values.

Bi1	–Se1 × 4	2.943(2)	Bi2	–Se4 × 2	2.863(2)	Bi3	–Se5 × 2	2.867(2)
	–Se4 × 2	2.959(3)		–Se5	2.930(3)		–Se6	2.930(3)
				–Se2 × 2	3.060(2)		–Se2	3.034(3)
				–Se1	3.079(3)		–Se3 × 2	3.073(1)
Bi4	–Se7	2.856(3)	Bi5	–Se8	2.724(4)	Bi6	–Se10	2.751(4)
	–Se6 × 2	2.865(2)		–Se7 × 2	2.859(2)		–Se9 × 2	2.803(2)
	–Se2 × 2	3.058(2)		–Se1 × 2	3.100(2)		–Se11 × 2	3.259(2)
	–Se3	3.062(1)		–Se2	3.134(4)		–Se6 × 2	3.586(3)
							–Se7	4.015(3)
Bi7	–Se11	2.772(3)	Pb1	–Se8 × 2	2.861(3)	K1	–K1 × 2	2.093(1)
	–Se10 × 2	2.949(2)		–Se9	2.957(4)		–Se8	2.825(4)
	–Se11 × 2	2.958(2)		–Se10 × 2	3.257(3)		–Se9	3.250(3)
	–Se5	3.093(3)		–Se4 × 2	3.526(3)		–Se7	3.496(3)
				–Se1	3.741(4)		–Se8 × 2	3.516(3)
							–Se9 × 2	3.856(3)
							–Se7	4.075(3)
Se1	–Bi1 × 2	2.943(2)	Se2	–Bi3	3.034(3)	Se3	–Bi3 × 4	3.062(1)
	–Bi2	3.079(3)		–Bi4 × 2	3.058(2)		–Bi4 × 2	3.073(1)
	–Bi5 × 2	3.100(2)		–Bi2 × 2	3.060(2)			
	–Pb1	3.741(4)		–Bi5	3.134(3)			
Se4	–Bi2 × 2	2.863(2)	Se5	–Bi3 × 2	2.867(2)	Se6	–Bi4 × 2	2.865(2)
	–Bi1	2.959(3)		–Bi2	2.930(3)		–Bi3	2.930(3)
	–Se10	3.526(3)		–Bi7	3.093(3)		–Se11	3.487(4)
	–Pb1 × 2	3.573(4)					–Bi6 × 2	3.586(3)
Se7	–Bi4	2.856(3)	Se8	–Bi5	2.724(4)	Se9	–Bi6 × 2	2.803(2)
	–Bi5 × 2	2.859(2)		–K1	2.825(4)		–Pb1	2.957(4)
	–K1	3.496(4)		–Pb1 × 2	2.861(3)		–K1	3.250(3)
	–Se9 × 2	3.962(4)		–K1 × 2	3.516(3)		–Se8 × 2	3.581(4)
	–Se8 × 2	3.978(4)		–Se9 × 2	3.581(4)		–Se10 × 2	3.815(4)
	–Bi6	4.015(3)		–Se7 × 2	3.978(4)		–K1 × 2	3.865(3)
							–Se7 × 2	3.962(4)
Se10	–Bi6	2.751(4)	Se11	–Bi7	2.772(3)			
	–Bi7 × 2	2.949(2)		–Bi7 × 2	2.958(2)			
	–Pb1 × 2	3.257(3)		–Bi6 × 2	3.259(2)			
	–Se4	3.573(4)		–Se6	3.487(4)			
	–Se9 × 2	3.815(4)						

Table 7. Fractional atomic coordinates ($y = 0$) and equivalent atomic displacement parameter (U_{eq})[a] values in 10^{-3} Å^2 for $Rb_{0.69}Pb_{3.69}Bi_{11.31}Se_{21}$ [b] with estimated standard deviations in parentheses.

	x	z	occupancy	U_{eq}
Bi1	0.5	0.5	1	18.7(3)
Bi/Pb2[c]	0.03035(3)	0.72151(6)	1	18.9(2)
Bi/Pb3[c]	0.44434(3)	0.04938(6)	1	20.0(2)
Bi4	0.07659(3)	0.17211(6)	1	17.3(2)
Bi5	0.39809(3)	0.60809(6)	1	20.9(3)
Bi6	0.22032(4)	0.19270(7)	1	26.3(3)
Bi7	0.19850(3)	0.91787(6)	1	21.0(3)
Pb/Bi1′[c]	0.15457(5)	0.64067(8)	1	42.5(4)
Rb1	0.2468(4)	0.4965(8)	0.69(2)	132(8)
Se1	0.04918(9)	0.4503(2)	1	20.4(6)
Se2	0.47922(8)	0.7910(1)	1	16.8(6)
Se3	0	0	1	18.0(8)
Se4	0.42687(9)	0.3329(2)	1	19.7(6)
Se5	0.09699(9)	0.8916(1)	1	23.0(6)
Se6	0.37817(9)	0.8777(2)	1	19.7(6)
Se7	0.14407(9)	0.3363(2)	1	18.3(6)
Se8	0.3292(1)	0.4554(2)	1	35.0(8)
Se9	0.25432(9)	0.6921(2)	1	22.2(6)
Se10	0.30880(8)	0.2052(1)	1	17.6(6)
Se11	0.29159(8)	0.9566(2)	1	16.9(6)

[a] U_{eq} is defined as one-third of the trace of the orthogonalized U_{ij} tensor. [b] Formula obtained according to charge balance requirements of the general formula $Rb_{1-x}Pb_{4-x}Bi_{11+x}Se_{21}$. [c] Bond-valence calculations indicate that this position is most likely mixed occupied with Bi and Pb. Bi/Pb2 = 2.80, Bi/Pb3 = Bi/Pb3 = 2.78, Pb/Bi1′ = 2.46.

diffractometer equipped with a position-sensitive detector. The purity and homogeneity was confirmed by comparing the X-ray powder diffraction pattern to that calculated from single-crystal data by using the CERIUS^2 software.[18]

Single-crystal X-ray crystallography: Single crystals of $K_{1-x}Sn_{4-x}Bi_{11+x}Se_{21}$, $K_{1-x}Pb_{4-x}Bi_{11+x}Se_{21}$, $Rb_{1-x}Pb_{4-x}Bi_{11+x}Se_{21}$, and $Cs_{1-x}Pb_{4-x}Bi_{11+x}Se_{21}$ were mounted on the tip of a glass fiber. The intensity data were collected on a Siemens SMART Platform CCD diffractometer with graphite monochromatized $Mo_{K\alpha}$ radiation and the SMART software[19] for data acquisition. The extraction and reduction of the data were performed with the program SAINT.[20] The observed systematic absences led to the space group $C2/m$. An analytical absorption correction using the program XPREP[21] was followed by a semi-empirical absorption correction based on symmetrically equivalent reflections that was done for each data set with the program SADABS.[22] The crystal structures were solved with direct methods (SHELXS-97[21]). All structure refinements were performed using the SHELXTL package of crystallographic programs.[21]

Twenty crystallographically independent positions (Bi1–7, M1, Se1–11, and A1) were found situated on mirror planes ($y = 0$ and 1/2). This gives the ideal charge-balanced formula $AM_4Bi_{11}Se_{21}$ assuming A^{+1}, M^{+2}, Bi^{+3}, and Se^{-2}. The elemental composition (determined by EDS), charge balance requirements, and anomalous thermal atomic displacement parameters (ADPs) occurring in all refinements of the isostructural compounds indicated site occupancy disorder of the metal atoms.

$K_{0.54}Sn_{3.54}Bi_{11.46}Se_{21}$: The structure refinement revealed relatively high thermal displacement parameters for the Bi3, and Bi5–Bi7 sites; therefore we introduced a disorder model with mixed Bi/Sn occupancies for these sites. In contrast, a small thermal displacement parameter of the Sn1 site indicated higher electron density on this site. This led to a disorder model of

Table 8. Selected interatomic distances [Å] for $Rb_{0.69}Pb_{3.69}Bi_{11.31}Se_{21}$. Because of the mixed Bi/Pb occupancy on all metal sites, these distances represent only average values.

Bi1	–Se1 × 4	2.945(2)	Bi2	–Se4 × 2	2.859(2)	Bi3	–Se5 × 2	2.874(2)
	–Se4 × 2	2.962(2)		–Se5	2.920(3)		–Se6	2.936(3)
				–Se2 × 2	3.075(2)		–Se2	3.036(2)
				–Se1	3.105(3)		–Se3 × 2	3.081(1)
Bi4	–Se7	2.856(3)	Bi5	–Se8	2.734(3)	Bi6	–Se10	2.754(3)
	–Se6 × 2	2.866(2)		–Se7 × 2	2.857(2)		–Se9 × 2	2.804(2)
	–Se2 × 2	3.062(2)		–Se1 × 2	3.099(2)		–Se11 × 2	3.255(2)
	–Se3	3.067(1)		–Se2	3.140(2)		–Se6 × 2	3.588(2)
							–Se7	4.118(3)
Bi7	–Se11	2.790(3)	Pb1	–Se8 × 2	2.856(3)	Rb1	–Rb1 × 2	2.106(2)
	–Se10 × 2	2.949(2)		–Se9	2.966(3)		–Se8	2.99(2)
	–Se11 × 2	2.963(2)		–Se10 × 2	3.258(2)		–Se9	3.33(1)
	–Se5	3.100(3)		–Se4 × 2	3.510(3)		–Se7	3.40(1)
				–Se1	3.721(3)		–Se8 × 2	3.54(1)
							–Se9 × 2	3.90(1)
							–Se7 × 2	4.16(1)
Se1	–Bi1 × 2	2.945(2)	Se2	–Bi3	3.036(2)	Se3	–Bi4 × 2	3.067(1)
	–Bi5 × 2	3.099(2)		–Bi4 × 2	3.062(2)		–Bi3 × 4	3.081(1)
	–Bi2	3.105(3)		–Bi2 × 2	3.075(2)			
	–Pb1	3.721(3)		–Bi5	3.140(2)			
Se4	–Bi2 × 2	2.859(2)	Se5	–Bi3 × 2	2.874(2)	Se6	–Bi4 × 2	2.866(2)
	–Bi1	2.961(4)		–Bi2	2.920(3)		–Bi3	2.937(3)
	–Pb1 × 2	3.510(3)		–Bi7	3.100(3)		–Se11	3.536(4)
	–Se10	3.577(4)					–Bi6 × 2	3.587(2)
Se7	–Bi4	2.856(3)	Se8	–Bi5	2.735(3)	Se9	–Bi6 × 2	2.804(2)
	–Bi5 × 2	2.857(2)		–Pb1 × 2	2.857(3)		–Pb1	2.966(3)
	–Rb1	3.40(1)		–Rb1	2.90(2)		–Rb1	3.33(1)
	–Se8 × 2	3.999(3)		–Se9 × 2	3.592(3)		–Se8 × 2	3.592(3)
				–Rb1 × 2	3.54(1)		–Se10 × 2	3.805(4)
				–Se7 × 2	3.999(3)		–Rb1 × 2	3.90(1)
Se10	–Bi6	2.754(3)	Se11	–Bi7	2.790(3)			
	–Bi7 × 2	2.948(2)		–Bi7 × 2	2.963(2)			
	–Pb1 × 2	3.258(2)		–Bi6 × 2	3.255(2)			
	–Se4	3.577(4)		–Se6	3.536(4)			
	–Se9 × 2	3.805(4)		–Se10 × 2	3.969(3)			
	–Se11 × 2	3.969(3)						

Table 9. Fractional atomic coordinates ($y = 0$) and equivalent atomic displacement parameter (U_{eq})[a] values in 10^{-3} Å^2 for $Cs_{0.65}Pb_{3.65}Bi_{11.35}Se_{21}$[b] with estimated standard deviations in parentheses.

	x	z	occupancy	U_{eq}
Bi/Pb1[c]	0.5	0.5	1	13.7(3)
Bi/Pb2[c]	0.03053(3)	0.72200(5)	1	10.9(2)
Bi/Pb3[c]	0.44421(3)	0.04952(5)	1	12.0(2)
Bi/Pb4[c]	0.07665(3)	0.17129(5)	1	10.5(2)
Bi5	0.39884(3)	0.60987(5)	1	15.2(2)
Bi/Pb6[c]	0.22112(3)	0.19283(5)	1	18.5(2)
Bi7	0.19835(3)	0.91768(5)	1	13.0(2)
Pb/Bi1′[c]	0.15362(4)	0.63990(6)	1	34.0(3)
Cs1	0.2489(2)	0.4960(4)	0.65(1)	90(3)
Se1	0.04884(7)	0.4492(1)	1	13.1(5)
Se2	0.47925(7)	0.7817(1)	1	8.6(4)
Se3	0	0	1	9.0(6)
Se4	0.42670(7)	0.3332(1)	1	12.5(4)
Se5	0.09760(7)	0.8919(1)	1	14.9(5)
Se6	0.37754(7)	0.8779(1)	1	12.0(4)
Se7	0.14407(7)	0.3360(1)	1	12.4(4)
Se8	0.3310(1)	0.4561(2)	1	37.5(8)
Se9	0.25268(8)	0.6916(1)	1	15.8(5)
Se10	0.30906(7)	0.2055(1)	1	11.6(5)
Se11	0.29098(7)	0.9563(1)	1	10.3(4)

[a] U_{eq} is defined as one-third of the trace of the orthogonalized U_{ij} tensor. [b] Formula obtained according to charge balance requirements of the general formula $Cs_{1-x}Pb_{4-x}Bi_{11+x}Se_{21}$. [c] Bond-valence calculations indicate that this position is most likely mixed occupied with Bi and Pb. Bi/Pb1 = 2.85, Bi/Pb2 = 2.71, Bi/Pb3 = 2.70, Bi/Pb4 = 2.85, Bi/Pb6 = 2.89, Pb/Bi1′ = 2.49.

Sn and Bi occupying this site. The refinement resulted in 15 % Sn in the Bi3 site, 18 % Sn in the Bi5 site, 34 % Sn in the Bi6 site, 25 % Sn in the Bi7 site, and 16 % Bi in the Sn1 site. The thermal displacement parameter of the K1 site remained high with 248 Å^2 after the refinement of the occupancy of this site that converged to 0.27(2), that is, equal to 1/4 occupied. The final formula $K_{0.54}Sn_{3.54}Bi_{11.46}Se_{21}$ was obtained by restraining the occupancies to be charge balanced. After anisotropic refinement the $R1$ and $wR2$ values dropped from 7.5 % and 13.0 % to 5.4 % and 9.6 %, respectively. The results of the structure refinement and other crystallographic data are given in Tables 2, 3, and 4.

$K_{1.46}Pb_{3.08}Bi_{11.46}Se_{21}$: Bi and Pb are not distinguishable by X-rays therefore the disorder model of $K_{0.54}Sn_{3.54}Bi_{11.46}Se_{21}$ was applied as a starting point to the lead compound. Furthermore, we refined the sites Bi1 – 7 and Pb1 as fully occupied with Bi or Pb, respectively, although charge balance requires mixed occupancies with Bi and Pb for several metal sites. Relatively high thermal displacement parameters of the Bi6 – 7 and Pb1 sites lead to refinement of the occupancy of these sites; this caused a significant drop of the R values from 6.2 % and 13.2 % to 5.8 % and 12.2 %, respectively. This introduced a disorder model with Pb and K occupying the same site. The refinement converged with the following mixed occupancies, Bi5 (11 % K), Bi6 (15 % K), and Pb1 (10 % K). The final formula $K_{1.46}Pb_{3.08}Bi_{11.46}Se_{21}$ was obtained according to charge-balance requirements. Several Bi sites must contain Pb to fulfill this requirement. Valence-bond calculations indicate that the positions Bi2, Bi3, and Pb1 are most likely to have mixed occupancies (VaList program available from ftp://ftp.ill.fr/pub/dif/valist). An elongated shape of the diffraction spots indicated twinning, which probably caused the residual electron density of 11.85 e Å^{-3} 1.59 Å away from Se10 and a higher $wR2$ than the other structure refinements. The results of the structure refinement and other crystallographic data are given in Tables 2, 5, and 6.

0947-6539/01/0709-1924 $ 17.50+.50/0 *Chem. Eur. J.* **2001**, *7*, No. 9

$Rb_{0.69}Pb_{3.69}Bi_{11.31}Se_{21}$: A high thermal displacement parameter of Rb1 indicated a statistical disorder of the alkali metal similar to the K compounds. The structure refinement converged at a partial Rb occupancy of 0.343(10) equal to about 1/3 occupied. Charge balance according to the general formula $Rb_{1-x}Pb_{4-x}Bi_{11+x}Se_{21}$ requires mixed occupancies with Bi and Pb for several sites, but they cannot be refined by means of X-ray measurements. Valence-bond calculations suggest that the Bi2, Bi3, and Pb1 sites have mixed Bi and Pb occupancies. The results of the structure refinement and other crystallographic data are given in Tables 2, 7, and 8.

$Cs_{0.65}Pb_{3.65}Bi_{11.35}Se_{21}$: A high thermal displacement parameter of the Cs1 site followed the same disorder model as for the above described compounds. The final refinement, constrained with charge balance requirements, gave $Cs_{1-x}Pb_{4-x}Bi_{11+x}Se_{21}$ withc $x \approx 0.35$. According to valence-bond calculations the Bi1 – 4, Bi6 and Pb1 sites are most likely to have mixed Bi and Pb occupancies. The results of the structure refinement and other crystallographic data are given in Tables 2, 9, and 10.

Further details on the crystal structure investigations may be obtained from the Fachinformationszentrum Karlsruhe, D-76344 Eggenstein-Leopoldshafen, Germany (fax: (+49) 7247-808-666; e-mail: crysdata@fiz-karlsruhe.de), on quoting the depository numbers CSD-411653 ($Cs_{0.65}Pb_{3.65}Bi_{11.35}Se_{21}$), CSD-411654 ($K_{1.46}Pb_{3.08}Bi_{11.46}Se_{21}$), CSD-411655 ($K_{0.54}Sn_{3.54}Bi_{11.46}Se_{21}$) and CSD-411656 ($Rb_{0.69}Pb_{3.69}Bi_{11.31}Se_{21}$).

Acknowledgements

Financial support from the Office of Naval Research (Grant No. N00014-98-1-0443) and the Deutsche Forschungsgemeinschaft is gratefully acknowledged. This work made use of the SEM facilities of the Center for Advanced Microscopy at Michigan State University.

[1] a) G. A. Slack in *CRC Handbook of Thermoelectrics* (Ed.: D. M. Rowe), CRC, Boca Raton, **1995**, p. 407; b) G. A. Slack, *Solid State Phys.* **1997**, *34*, 1; c) B. C. Sales, *Mater. Res. Bull.* **1998**, *23*, 15; d) B. C. Sales, D. Mandrus, B. C. Chakoumakos, V. Keppens, J. R. Thompson, *Phys. Rev. B.* **1997**, *56*, 15081; e) T. M. Tritt, *Science* **1996**, *272*, 1276; f) M. G. Kanatzidis, F. J. DiSalvo, *ONR Q. Rev.* **1996**, *27*, 14; g) D.-Y. Chung, L. Iordanidis, K.-S. Choi, M. G. Kanatzidis, *Bull. Korean Chem. Soc* **1998**, *19*, 1283; h) "The Role of Solid State Chemistry in the Discovery of New Thermoelectric Materials", M. G. Kanatzidis, in *Semiconductors and Semimetals*, Academic Press, **2000**.

[2] a) "Thermoelectric Materials 1998—The Next Generation Materials for Small-Scale Refrigeration and Power Applications", *Mater. Res. Soc. Symp. Proc.* **1998**, *545*, whole issue; b) "Thermoelectric Materials—New Directions and Approaches", *Mater. Res. Soc. Symp. Proc.* **1998**, *478*, whole issue.

[3] *CRC Handbook of Thermoelectrics* (Ed.: D. M. Rowe), CRC, Boca Raton, **1995**.

[4] a) H.-H. Jeon, H.-P. Ha, D.-B. Hyun, J.-D. Shim, *J. Phys. Chem. Solids* **1991**, *4*, 579; b) L. R. Testardi, J. N. Bierly, Jr., F. J. Donahoe, *J. Phys. Chem. Solids* **1962**, *23*, 1209; c) C. H. Champness, P. T. Chiang, P. Parekh, *Can. J. Phys.* **1965**, *43*, 653; d) C. H. Champness, P. T. Chiang, P. Parekh, *Can. J. Phys.* **1967**, *45*, 3611; e) M. V. Vedernikov, V. A. Kutasov, L. N. Lukyanova, P. P. Konstantinov, *Proc. 16th Int. Conf. On Thermoelectrics* (Dresden, Germany) **1997**, p. 56; f) M. Stordeur in *CRC Handbook of Thermoelectrics* (Ed.: D. M. Rowe), CRC Press, Boca Raton **1995**, p. 239.

[5] D.-Y. Chung, T. Hogan, P. W. Brazis, M. Rocci-Lane, C. R. Kannewurf, M. Bastea, C. Uher, M. G. Kanatzidis, *Science* **2000**, *287*, 1024.

[6] a) M. G. Kanatzidis, D.-Y. Chung, L. Iordanidis, K.-S. Choi, P. Brazis, M. Rocci, T. Hogan, C. Kannewurf, *Mat. Res. Soc. Symp. Proc.* **1998**,

Table 10. Selected interatomic distances [Å] for $Cs_{0.65}Pb_{3.65}Bi_{11.35}Se_{21}$. Because of the mixed Bi/Pb occupancy on all metal sites, these distances represent only average values.

Bi1	–Se1 × 4	2.945(2)	Bi2	–Se4 × 2	2.870(2)	Bi3	–Se5 × 2	2.883(2)
	–Se4 × 2	2.974(2)		–Se5	2.935(2)		–Se6	2.954(2)
				–Se2 × 2	3.088(2)		–Se2	3.042(2)
				–Se1	3.111(2)		–Se3 × 2	3.0933(6)
Bi4	–Se7	2.874(2)	Bi5	–Se8	2.745(3)	Bi6	–Se10	2.765(2)
	–Se6 × 2	2.877(2)		–Se7 × 2	2.863(2)		–Se9 × 2	2.805(2)
	–Se3	3.0732(8)		–Se1 × 2	3.105(2)		–Se11 × 2	3.254(2)
	–Se2 × 2	3.074(1)		–Se2	3.133(2)		–Se6 × 2	3.607(2)
							–Se7	4.167(2)
Bi7	–Se11	2.803(2)	Pb1	–Se8 × 2	2.844(2)	Cs1	–Cs1 × 2	2.0858(4)
	–Se10 × 2	2.948(2)		–Se9	2.972(3)		–Se8	3.003(4)
	–Se11 × 2	2.963(2)		–Se10 × 2	3.265(2)		–Se9	3.334(2)
	–Se5	3.110(2)		–Se4 × 2	3.501(2)		–Se7	3.523(2)
				–Se1	3.734(3)		–Se8 × 2	3.656(3)
							–Se9 × 2	3.932(2)
							–Se7 × 2	4.094(2)
Se1	–Bi1 × 2	2.945(2)	Se2	–Bi3	3.042(2)	Se3	–Bi4 × 2	3.0732(8)
	–Bi5 × 2	3.104(2)		–Bi4 × 2	3.074(2)		–Bi3 × 4	3.0934(6)
	–Bi2	3.111(2)		–Bi2 × 2	3.088(2)			
	–Pb1	3.734(3)		–Bi5	3.133(2)			
Se4	–Bi2 × 2	2.870(2)	Se5	–Bi3 × 2	2.883(2)	Se6	–Bi4 × 2	2.877(2)
	–Bi1	2.974(2)		–Bi2	2.935(2)		–Bi3	2.954(2)
	–Pb1 × 2	3.501(2)		–Bi7	3.110(2)		–Se11	3.565(3)
	–Se10	3.593(3)					–Bi6 × 2	3.607(2)
Se7	–Bi5 × 2	2.863(2)	Se8	–Bi5	2.745(3)	Se9	–Bi6 × 2	2.805(2)
	–Bi4	2.874(2)		–Pb1 × 2	2.844(2)		–Pb1	2.972(3)
	–Cs1	3.523(2)		–Cs1	3.003(4)		–Cs1	3.334(2)
	–Se8 × 2	4.009(3)		–Se9 × 2	3.604(3)		–Se8 × 2	3.604(3)
				–Cs1 × 2	3.656(3)		–Se10 × 2	3.794(3)
				–Se7 × 2	4.009(3)		–Cs1 × 2	3.933(2)
Se10	–Bi6	2.765(2)	Se11	–Bi7	2.803(2)			
	–Bi7 × 2	2.948(2)		–Bi7 × 2	2.962(2)			
	–Pb1 × 2	3.265(2)		–Bi6 × 2	3.254(2)			
	–Se4	3.593(3)		–Se6	3.565(3)			
	–Se9 × 2	3.794(3)		–Se10 × 2	3.975(3)			
	–Se11 × 2	3.975(3)						

545, 233; b) P. W. Bravis, M. A. Rocci-Lane, J. R. Ireland, D.-Y. Chung, M. G. Kanatzidis, C. R. Kannewurf, *Proc. 18th Int. Conf. On Thermoelectrics* (Baltimore, USA) **1999**, p. 619.

[7] a) M. G. Kanatzidis, T. J. McCarthy, T. A. Tanzer, L.-H. Chen, L. Iordanidis, T. Hogan, C. R. Kannewurf, C. Uher, B. Chen, *Chem. Mater.* **1996**, *8*, 1465; b) B. Chen, C. Uher, L. Iordanidis, M. G. Kanatzidis, *Chem. Mater.* **1997**, *9*, 1655.

[8] K.-S. Choi, D.-Y. Chung, A. Mrotzek, P. Brazis, C. R. Kannewurf, C. Uher, W. Chen, T. Hogan, M. G. Kanatzidis, unpublished results.

[9] D.-Y. Chung, L. Iordanidis, K. K. Rangan, P. W. Brazis, C. R. Kannewurf, M. G. Kanatzidis, *Chem. Mater.* **1999**, *11*, 1352.

[10] L. Iordanidis, M. G. Kanatzidis, unpublished results.

[11] Y.-C. Wang, F. J. DiSalvo, *Chem. Mater.* **2000**, *12*, 1011.

[12] Y. Iitaka, W. Nowacki, *Acta Crystallogr.* **1962**, *15*, 691.

[13] A. Mrotzek, D-Y. Chung, T. Hogan, M. G. Kanatzidis, *J. Mater. Chem.* **2000**, *10*, 1.

[14] The coordination environment of the Se atoms ranges from three to six. The relatively high isotropic displacement parameters of Se8 (37 Å^3) and Se9 (29 Å^3) may be explained with the lower and mixed occupancy of the K1 and the Sn1 sites, respectively. Especially the bond length Se8 – K1 (2.56 Å) is shorter than usual, also the Sn1 – Se8/9 bond lengths are the shortest observed (compare Table 5); this is due to the large fraction of the smaller Sn on the Sn1 site. The following relaxation of the structure might be possible. If K atoms are absent, Se8 and Se9 could be pushed away when binding to a Bi atom on the Sn1 site; this requires longer interatomic M – Se distances. When K atoms are present Se8 and Se9 might move closer to the Sn1 site and could create shorter Sn1 – Se bond lengths that are more suitable for a Sn atom. This fluctuation could give rise to a superstructure. Probably the individual tunnels in the structure are too remote to communicate, therefore high displacement parameters are observed instead of possible ordering.

[15] D.-Y. Chung, K.-S. Choi, L. Iordanidis, J. L. Schindler, P. W. Brazis, C. R. Kannewurf, B. Chen, S. Hu, C. Uher, M. G. Kanatzidis, *Chem. Mater.* **1997**, *9*, 3060.

[16] T. Hogan, N. Ghelani, S. Loo, S. Sportouch, S.-J. Kim, D.-Y. Chung, M. G. Kanatzidis, *Proc. 18th Int. Conf. On Thermoelectrics* (Baltimore, USA) **1999**, p. 619.

[17] O. Maldonado, *Cryogenics* **1992**, *32*, 908.

[18] *CERIUS^2, Version 1.6*, Molecular Simulations, Cambridge (UK), **1994**.

[19] *SMART*, Siemens Analytical X-ray Systems, Madison, WI (USA), **1996**.

[20] *SAINT V-4*, Siemens Analytical X-ray Systems, Madison, WI (USA), **1994 – 1996**.

[21] *SHELXTL V-5*, G. M. Sheldrick, Siemens Analytical X-ray Systems, Madison, WI (USA), **1994**.

[22] *SADABS V-4*, Siemens Analytical X-ray Systems, Madison, WI, (USA), **1994 – 1996**.

Received: October 24, 2000 [F2822]

  0947-6539/01/0709-1926 $ 17.50+.50/0